Supplementary Materials

Supplementary Methods

Data sources and study population

We performed a nationwide retrospective analysis of confirmed chikungunya virus (CHIKV) cases reported in Brazil between January 2015 and December 2025. Individual-level surveillance records were obtained from the Sistema de Informação de Agravos de Notificação (SINAN) through DATASUS, the information technology department of Brazil's Unified Health System (Sistema Único de Saúde, SUS).[1] SINAN is the mandatory notification system for infectious diseases in Brazil and includes patient demographics such as age, sex, race or ethnicity, municipality of residence, dates of symptom onset, notification, and hospitalization, reported clinical manifestations, and final outcomes.

Analyses were restricted to confirmed chikungunya cases as defined by SINAN case classification criteria (n = 1,235,424); suspected and discarded notifications were excluded. No restriction by confirmation criterion was applied, so the analytic set comprises laboratory-confirmed (n = 462,849), clinically confirmed (n = 752,444), cases with confirmation criteria under investigation (n = 19,892), and cases with no recorded confirmation criterion (n = 239). Population denominators stratified by age and sex were obtained from intercensal estimates provided by the Brazilian Institute of Geography and Statistics.[2] Municipality boundary files from IBGE were used to define spatial adjacency for subsequent spatial analyses.[3] Because laboratory confirmation covers only a subset of notified cases, estimated at 13% to 62% of suspected cases in Brazil,[4] restricting to laboratory-confirmed records would have excluded most clinically confirmed disease and biased estimates toward municipalities with greater diagnostic capacity. Retaining all confirmed cases preserves geographic coverage, but means these analyses characterize the epidemiology of notified and confirmed disease rather than true infection incidence.

Data preprocessing and variable definition

Records with missing or invalid information on age or sex were excluded. Age was analyzed both continuously and in grouped categories. For survival analyses, age was grouped in ten-year intervals, with infants younger than 1 year as a separate category. For symptom analyses, broader age categories were used: younger than 15, 15 to 29, 30 to 44, 45 to 59, and 60 years or older.
Race or color was recorded in SINAN according to the IBGE self-declaration standard, which classifies individuals into five categories: *branca* (White), *preta* (Black), *amarela* (East Asian), *parda* (mixed ancestry, predominantly European-African-Indigenous combinations), and *indígena* (Indigenous).[5] The term pardo refers to individuals of mixed ancestry, predominantly European-African-Indigenous combinations, as defined by the IBGE self-declaration standard.[2] Following standard practice in Brazilian epidemiological research, preta and parda categories were aggregated into a single Black category for some analyses of racial disparities.[5] Race or color was

missing or recorded as ignored in 23.2% of confirmed case records; these individuals were excluded from race-stratified analyses but retained in all other analyses. Because missingness was more common in municipalities with lower case confirmation rates, race-specific estimates may understate inequities in access to care.

Municipality-level incidence, hospitalization, and death rates were calculated as the number of events per 100,000 population, aggregated at the temporal resolution appropriate to each analysis. For analyses of disease progression, three time-to-event intervals were defined in days: symptom onset to hospitalization, hospitalization to death, and symptom onset to death. Individuals who did not experience the event of interest during follow-up were right censored at the last observed date.

Descriptive epidemiological analyses

National and regional temporal trends were summarized using weekly aggregated case counts and population-standardized incidence rates. Seasonal patterns were explored using weekly moving averages and deviations from long-term weekly means. Annual age and sex distributions of reported cases were summarized using boxplots. Differences across race and ethnicity groups were summarized using annual incidence rates and proportional distributions. Municipality-level sex differences in case burden were evaluated by comparing the proportion of female and male cases, with statistical significance assessed using binomial tests and visualized using volcano-style plots.

Wavelet analysis of temporal periodicity

To characterize the temporal periodicity of chikungunya transmission, we applied a continuous wavelet transform to national monthly chikungunya case counts from January 2015 to December 2025. Monthly case counts were aggregated at the national level based on notification dates. Wavelet power spectra were computed using the Morlet wavelet function, which provides balanced resolution in time and frequency and is widely used for epidemiological time-series analysis.[6] Periods ranging from 2 months to 5 years were evaluated. Statistical significance was assessed against an AR(1) red-noise background spectrum, which represents the null hypothesis that observed power reflects autocorrelated background noise rather than a genuine periodic signal.[6] Significance contours were drawn at the 1% level, indicating periods where wavelet power significantly exceeded the red-noise expectation. To account for boundary effects inherent to finite time series, results outside the cone of influence were excluded from interpretation. Wavelet analyses were performed in R using the *WaveletComp* package.

Clinical symptom co-occurrence

To describe the clinical heterogeneity of reported cases, we examined the co-occurrence of reported symptoms among chikungunya cases. Common symptoms included fever, arthralgia, myalgia, headache, rash, vomiting, conjunctivitis, and leukopenia. Overlapping symptom profiles were visualized using an UpSet plot framework to highlight common multi-symptom combinations.

Survival analyses

Time-to-event outcomes were analyzed using Kaplan-Meier methods, stratified by age group, sex, and race or ethnicity, with differences assessed using log-rank tests. Three separate univariable Cox proportional hazards models were fitted, one each for age group, sex, and race or ethnicity, to estimate unadjusted associations between each demographic characteristic and disease progression. Because the aim was to characterize population-level demographic gradients in disease progression rather than to identify independent predictors, Cox models were fitted univariably. Results are reported as hazard ratios with 95% confidence intervals. Proportional hazards assumptions were evaluated using Schoenfeld residuals.

Municipality-level delay analyses

Spatial heterogeneity in disease progression and surveillance was assessed by calculating municipality-level median delays for key intervals, including symptom onset to notification and symptom onset to hospitalization. Median values were used to reduce sensitivity to extreme observations. Municipalities with insufficient numbers of events were excluded. Results were visualized using choropleth maps.

Bayesian spatiotemporal model

Municipality-level chikungunya case counts were analyzed using a Bayesian hierarchical spatiotemporal model implemented within the Integrated Nested Laplace Approximation framework. Let Y_{it} denote the number of reported chikungunya cases in municipality during month. The outcome was assumed to follow a Poisson distribution. A log link function was used, with municipality population size included as an offset.

The linear predictor included an intercept, a standardized national monthly Zika incidence covariate, spatial random effects, a temporal random effect, and a space-time interaction term. The structured spatial component was modeled using the Besag-York-Mollié 2 parameterization,[7] with an intrinsic conditional autoregressive prior defined on a first-order queen contiguity adjacency structure. The parameter ϕ represents the proportion of total spatial variance attributable to the structured spatial component, with values close to 1 indicating strong spatial autocorrelation and values near 0 indicating predominantly unstructured spatial heterogeneity. Temporal variation was

captured using a second-order random walk, and residual municipality-specific deviations were modeled through an unstructured space-time interaction term.

To assess whether the space-time interaction term exhibited spatial clustering beyond the structured spatial component, we computed Global Moran's I for each monthly time step using first-order queen contiguity weights.[8] To characterize persistent clustering at the municipality level, we also computed Local Indicators of Spatial Association using the time-averaged posterior mean of the interaction term.[9] Statistical significance was assessed at $p < 0.05$. To capture national-level co-circulation of arboviruses, we incorporated a time-varying covariate representing standardized national monthly Zika incidence. As a sensitivity analysis, the model was refit using a negative binomial likelihood to account for overdispersion in municipality-month case counts.[10] Full model specification:

$$Y_{it} \sim Poisson(\mu_{it}) \qquad \textit{(Equation 1)}$$

A log link function was used, with municipality population size included as an offset (Equation 2):

$$log(\mu_{it}) = log(POP_i) + \alpha + \beta Z_t + u_i + v_i + \gamma_t + \delta_{it} \qquad \textit{(Equation 2)}$$

The linear predictor represents the log incidence rate. Here, μ_{it} denotes the expected number of cases and POP_i represents the municipality population size included as an offset. The parameter α represents the overall intercept. The coefficient β represents the association between chikungunya incidence and the standardized national monthly Zika incidence covariate Z_t. Under this log-link model, exp(β) represents the multiplicative change in the chikungunya incidence rate associated with a one-standard-deviation increase in national Zika incidence, conditional on spatial, temporal, and spatiotemporal random effects.

Spatial effects

Spatial variation was modeled using the Besag-York-Mollié 2 (BYM2) parameterization.[7] The spatial random effect was decomposed into a structured component u_i and an unstructured component v_i. The structured spatial component u_i was modeled using an intrinsic conditional autoregressive (ICAR) prior defined on a first-order queen contiguity adjacency structure, such that municipalities sharing a common boundary or vertex were considered neighbors. Structured spatial effects were modeled using the BYM2 parameterization with an ICAR prior. This specification induces spatial smoothing by allowing geographically adjacent municipalities to exhibit similar underlying risk levels. The unstructured spatial component v_i captures spatially independent heterogeneity.

Temporal and space-time effects

Temporal variation was captured by γ_t, modeled using a second-order random walk (RW2) to impose smoothness in the temporal trend. Residual variability not explained by the additive spatial and temporal components was modeled using an unstructured space-time interaction term δ_{it}, allowing municipality-specific deviations from the overall temporal pattern.

Spatial autocorrelation analyses

To assess whether the space-time interaction term δ_{it} exhibited spatial clustering beyond the structured BYM2 component, we computed the Global Moran's I statistic for each monthly time step. For month *t*, let $x = \{\delta_{it}\}$ denote the vector of posterior means across all municipalities. The Global Moran's I is defined as (Equation 3):

$$I = \frac{N}{\sum_i \sum_j w_{ij}} \cdot \frac{\sum_i \sum_j w_{ij}(x_i - \bar{x})(x_j - \bar{x})}{\sum_i (x_i - \bar{x})^2} \qquad \textit{(Equation 3)}$$

Where *N* is the number of municipalities, w_{ij} are spatial weights from the first-order queen contiguity adjacency matrix (where w_{ij} = 1 if municipalities *i* and *j* share a common boundary or vertex, and 0 otherwise), *i* and *j* index individual municipalities and $\bar{x}$ is the spatial mean of δ_{it} at time *t*. Statistical significance was assessed under the assumption of normality, with $p < 0.05$ as the threshold.

To characterize persistent spatial clustering at the municipality level across the full study period, we additionally computed Local Indicators of Spatial Association (LISA) using the Local Moran's I statistic (Equation 4):

$$I_i = \frac{(x_i - \bar{x})}{s^2} \sum_j w_{ij}\left(x_j - \bar{x}\right) \qquad \textit{(Equation4)}$$

Where s^2 is the variance of *x*. LISA was applied to the time-averaged posterior mean of δ_{it}. Municipalities were classified into cluster types (HH, LL, HL, LH) based on the sign of I_i and the spatial lag $\Sigma\, w_{ij}\,(x_j - \bar{x})$ with significance defined at p < 0.05. All spatial autocorrelation analyses were performed using the spdep package in R.

National Zika covariate

To capture national-level co-circulation of arboviruses, we incorporated an external time-varying covariate Z_t representing standardized national monthly Zika incidence. Let C_t^Z denote the total number of confirmed Zika cases nationwide in month *t*, and let P^Z denote the total national population obtained by summing municipality-level population estimates. The raw national monthly Zika incidence rate (per 100,000) was computed as (Equation 5):

$$Z_t^{raw} = \frac{C_t^Z}{P^Z} \times 100{,}000 \qquad \textit{(Equation 5)}$$

To improve interpretability and numerical stability, the incidence rate was standardized across all months using a z-score transformation (Equation 6):

$$Z_t = \frac{Z_t^{\text{raw}} - \overline{Z^{\text{raw}}}}{\text{SD}(Z^{\text{raw}})} \qquad \textit{(Equation6)}$$

We used national Zika incidence rather than dengue as the arboviral covariate because Zika's temporally distinct emergence and epidemic peak provided a cleaner test of whether chikungunya spatial gradients simply mirrored broader arboviral surveillance pressure. Dengue's long-standing endemicity and overlapping seasonality with chikungunya would have introduced strong collinearity, making the covariate difficult to interpret mechanistically. The primary analytic goal was to assess independence of chikungunya spatial structure from co-circulating arboviral dynamics, for which Zika is the more appropriate probe.

Incidence rate definition

Rearranging Equation 2, the municipality-level incidence rate can be expressed as (Equation 7):

$$IR_{it} = \frac{\mu_{it}}{POP_i} = exp(\alpha + \beta Z_t + u_i + v_i + \gamma_t + \delta_{it}) \qquad \textit{(Equation 7)}$$

Incidence rates per 100,000 population were obtained by multiplying IR_{it} by 100,000.

Estimated incidence rate ratio definition

To quantify relative transmission intensity across municipalities, we defined a municipality-level posterior estimated incidence rate ratio (*IRR*) as the ratio between the model-estimated municipality incidence rate and the estimated national median municipality incidence rate at the same time point (Equation 8):

$$IRR_{it} = \frac{IR_{it}}{I\tilde{R}_t}$$

(Equation 8)

where IR_{it} denotes the model-estimated incidence rate for municipality *i* at time *t*, and $I\tilde{R}_t$ represents the national median of municipality-level incidence rates at time *t*. Equivalently (Equation 9):

$$log(IRR_{it}) = log(IR_{it}) - log(I\tilde{R}_t) \qquad \textit{(Equation 9)}$$

For visualization of regional trajectories, macro-regional summaries were computed as the median $log(IRR)$ across all municipalities within each macro-region at each time point.

Priors and inference

Penalized complexity (PC) priors were specified for precision parameters. Posterior inference was performed using INLA, which approximates marginal posterior distributions via Laplace approximation and numerical integration. Posterior municipality-level incidence rates were obtained by exponentiating the linear predictor after excluding the offset term. All analyses were conducted in R (version ≥4.2). Spatial analyses used the sf and spdep packages, Bayesian spatiotemporal models were fitted using INLA, and survival analyses used survival and survminer. All analyses were version controlled.

Municipality-level allocation framework

Each municipality with model estimates was assigned to a joint empirical tertile of recent (2024–25) posterior incidence rate ratio (IRR) and proportion of population aged 65 years or older from the IBGE 2022 census, yielding three policy zones: transmission-control priority (high IRR, lower elderly share), clinical-preparedness priority (lower IRR, high elderly share), and combined-priority (high on both dimensions). As a sensitivity analysis, the framework was reconstructed using cumulative 2015–25 posterior IRRs rather than the 2024–25 window; results are shown in Figure S7. The framework is intended as a planning heuristic and should be updated as surveillance data accumulate.

Supplementary Results

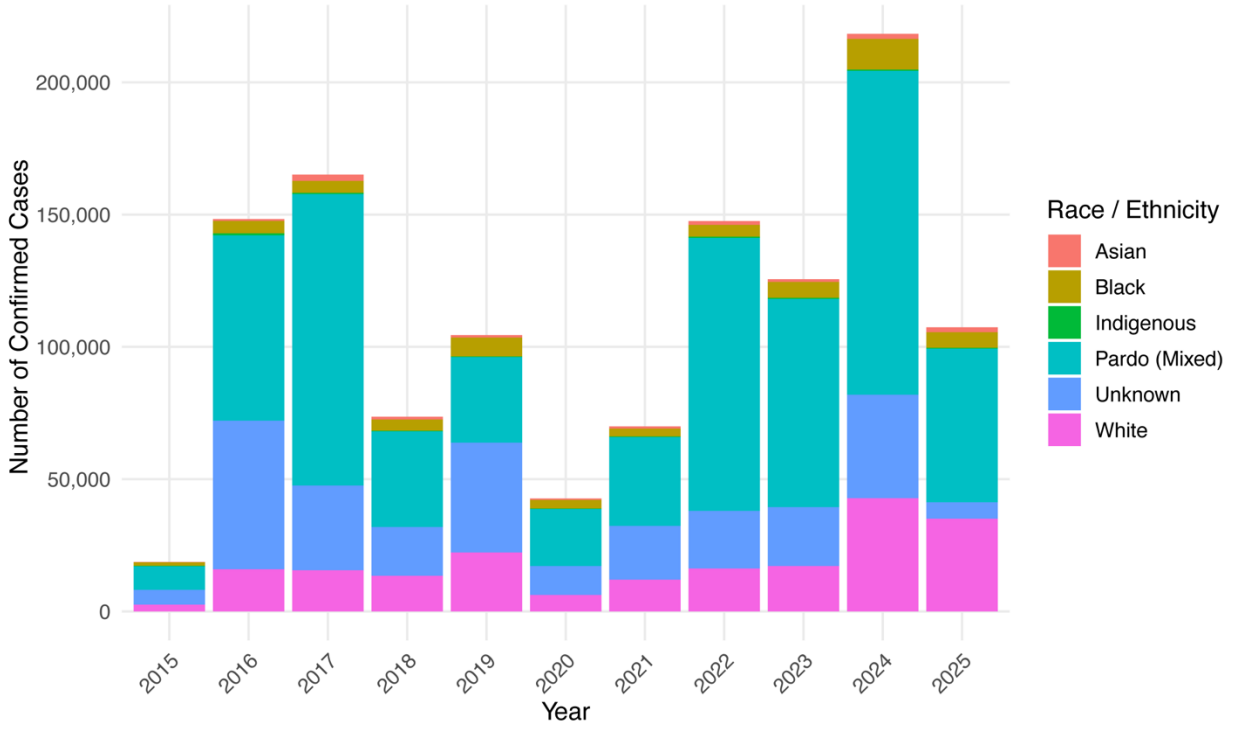

Figure S1. Annual number of confirmed chikungunya cases stratified by race or ethnicity from 2015 to 2025. Individuals classified as Pardo (mixed) consistently accounted for the largest share of reported cases across all years, followed by white and Black populations. Temporal fluctuations in total case counts reflect epidemic waves, while the relative contribution of each ethnic group remained broadly similar over time.

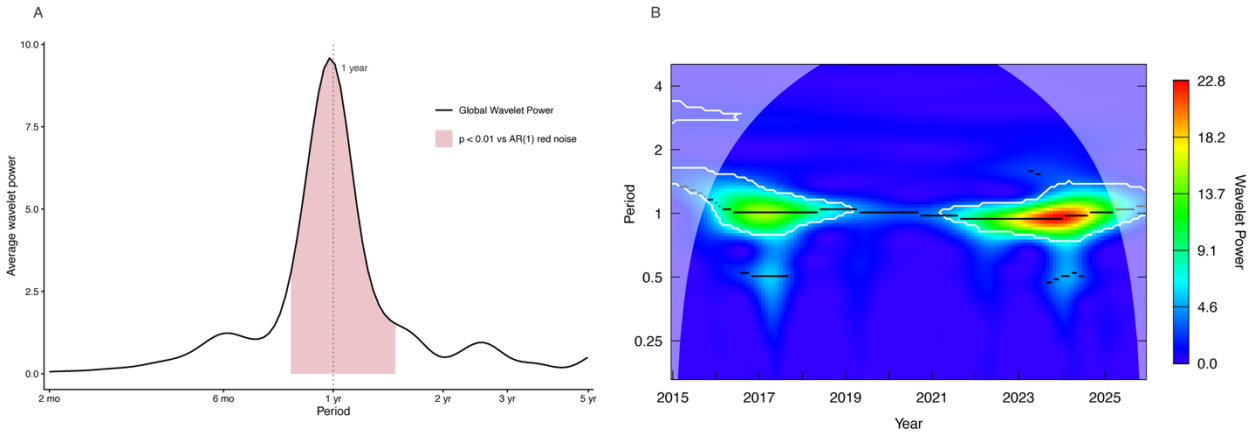

Figure S2. Wavelet power spectrum of national monthly chikungunya case counts, Brazil, 2015 to 2025. The continuous wavelet transform was computed using the Morlet wavelet applied to national monthly aggregated case counts. Color intensity indicates wavelet power at each combination of time (x-axis) and period (y-axis). The black contour encloses regions where power significantly exceeds a red-noise (autoregressive order-one) background at the 1% level, indicating genuine periodic signals rather than autocorrelated noise. A dominant annual cycle is present throughout the study period and is markedly amplified during the 2016 to 2017 and 2023 to 2024 epidemic waves. No sustained multi-year periodicity

was observed. The lighter shaded region at the edges indicates the cone of influence, where edge effects limit interpretation.

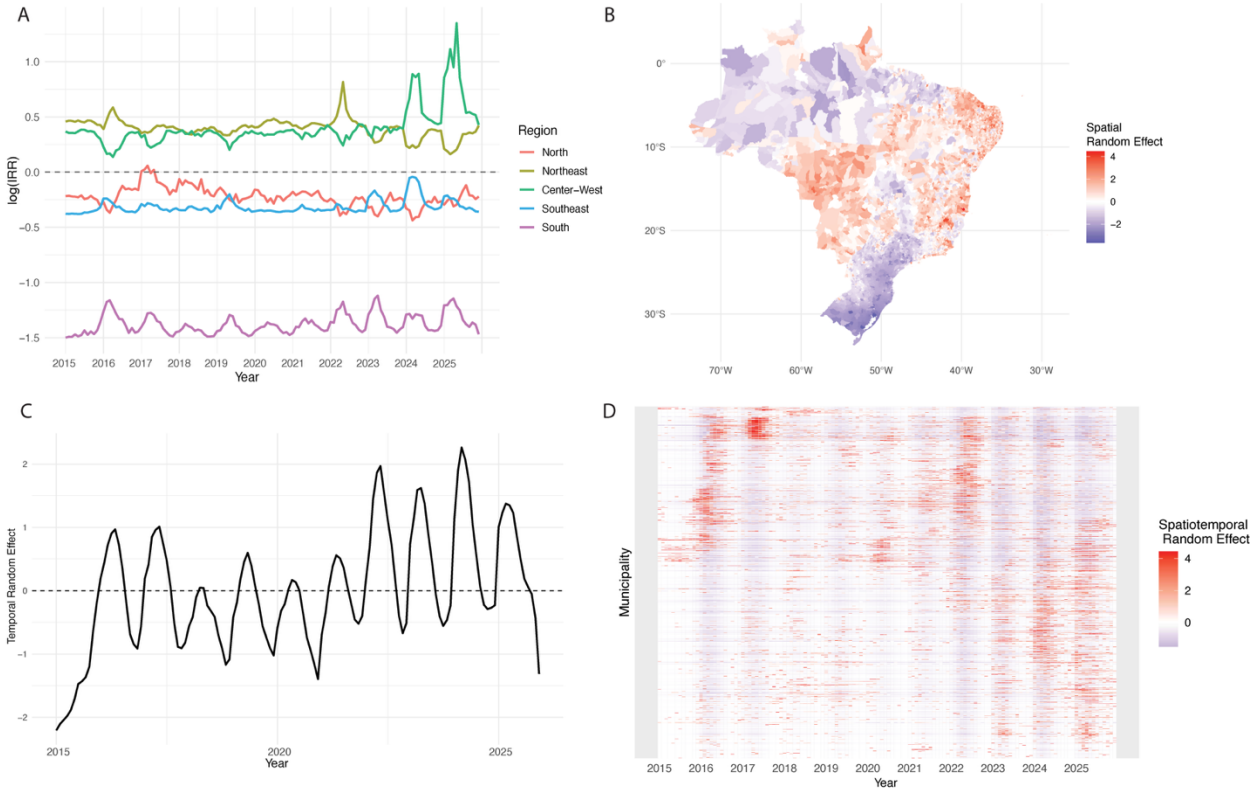

Figure S3. Decomposition of the Bayesian spatiotemporal model. (A) Monthly macro-regional log incidence rate ratios relative to the national municipality-median incidence. (B) Posterior mean of the spatial random effect (BYM2), representing persistent spatial structure after accounting for covariates and temporal trends. (C) Posterior mean of the temporal random effect (RW2), representing the national temporal trend after adjusting for spatial structure. (D) Posterior mean of the unstructured space-time interaction term, visualized as a municipality-by-month heatmap, capturing municipality-specific residual deviations beyond the additive spatial and temporal components.

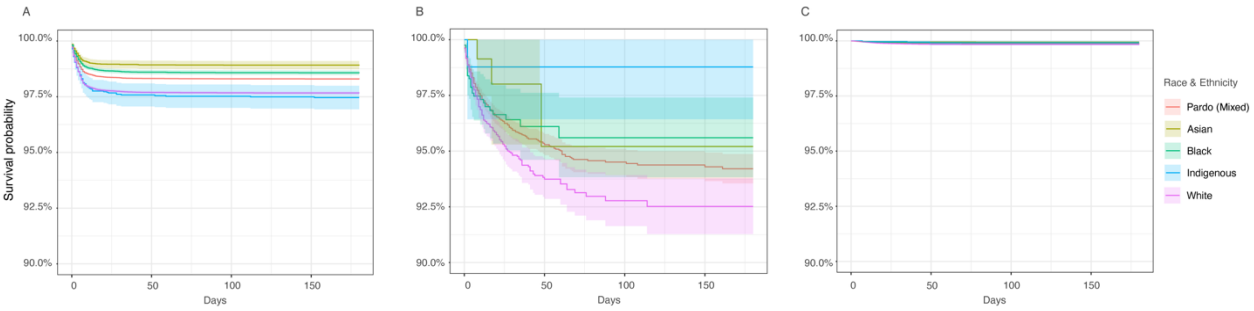

Figure S4. Kaplan-Meier survival estimates by race or ethnicity along the chikungunya clinical pathway, Brazil, 2015 to 2025. Survival estimates for three sequential clinical intervals stratified by race or ethnicity as classified per IBGE self-declaration categories (white, Black, Pardo, Asian, Indigenous). (A)

Symptom onset to hospitalization. (B) Hospitalization to death. (C) Symptom onset to death. Individuals with missing race or ethnicity (23.2% of records) were excluded. Differences were most pronounced for time from symptom onset to hospitalization, consistent with differences in access to care rather than intrinsic biological susceptibility. Shaded bands indicate 95% confidence intervals. Numbers at risk are shown below each panel.

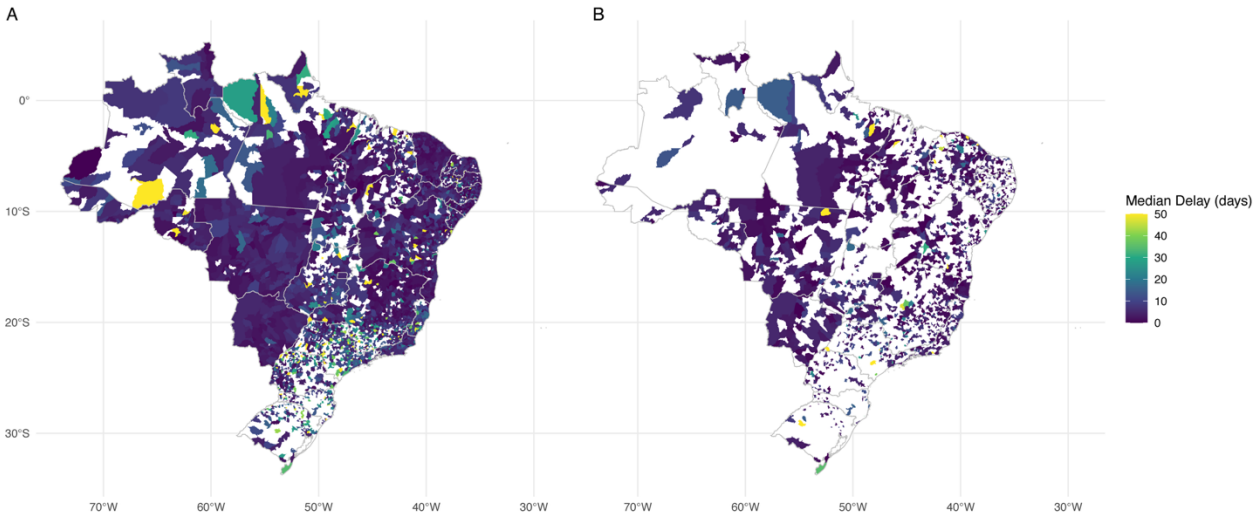

Figure S5. Municipality-level median delays in chikungunya notification and hospitalization, Brazil, 2015 to 2025. Choropleth maps show municipality-level median delays in days for two care-pathway intervals. (A) Symptom onset to notification. Median delays were generally short across most of Brazil but showed clusters of longer reporting times in parts of the North and South, which may reflect reduced confirmation capacity in those areas. (B) Symptom onset to hospitalization. Geographic heterogeneity was more pronounced, with longer median delays in parts of the North and Central-West. These patterns may reflect geographic variation in primary care access, referral pathways, and diagnostic capacity across SUS regions. Municipalities with fewer than five events were excluded to reduce instability in median estimates. Values are shown in days.

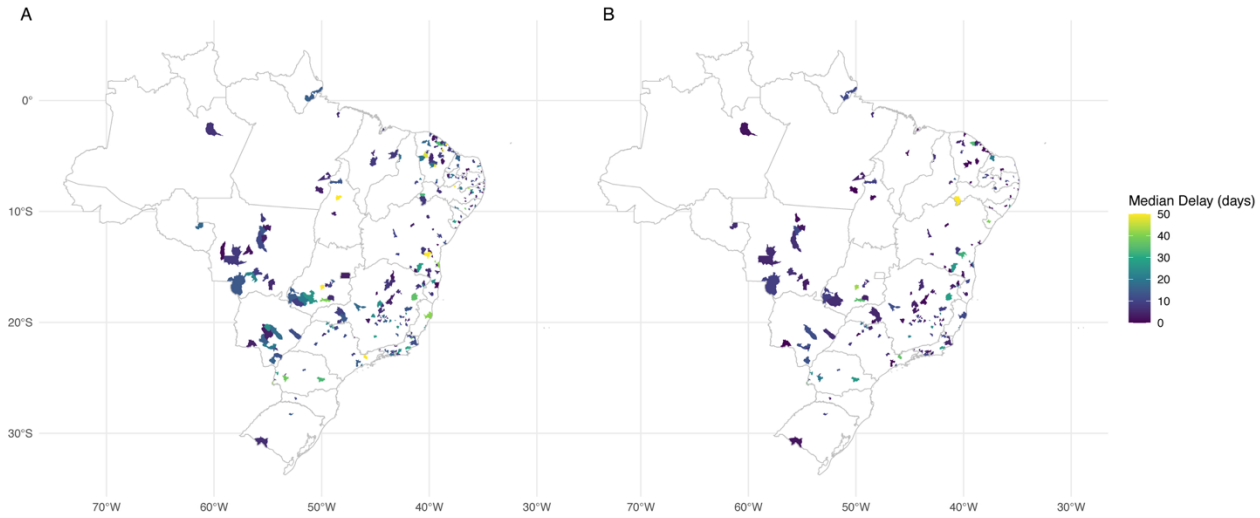

Figure S6. Municipality-level median time to death across the chikungunya clinical pathway. (A) Median time from symptom onset to death could be estimated only in a limited number of municipalities, reflecting the low frequency and uneven geographic distribution of fatal cases. (B) A similar pattern was observed for the median time from hospitalization to death, which was estimable in even fewer municipalities, consistent with the strong attrition of cases along the disease severity pathway.

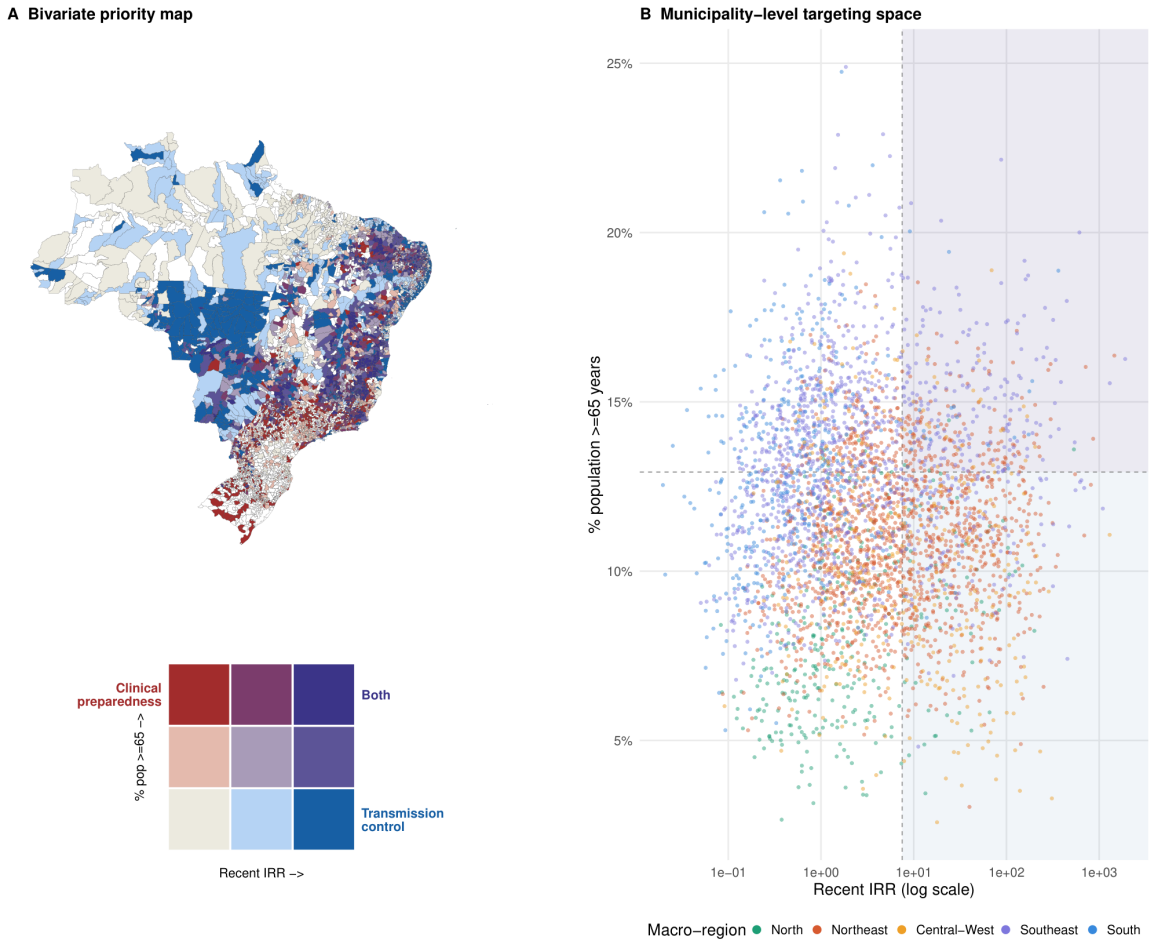

Figure S7. Combined geographic and demographic targeting using cumulative 2015 to 2025 IRRs, Brazil (sensitivity analysis). Sensitivity version of figure 6 constructed using cumulative posterior incidence rate ratios (IRRs) over the full 2015 to 2025 study period rather than the 2024 to 2025 window used in the main analysis. (A) Bivariate priority map and (B) municipality-level targeting space are constructed using identical joint empirical-tertile classification and the same IBGE 2022 proportion of population aged 65 years and older. The macro-regional distribution of priority zones is broadly concordant with figure 6, demonstrating the robustness of the targeting framework to the choice of time window.

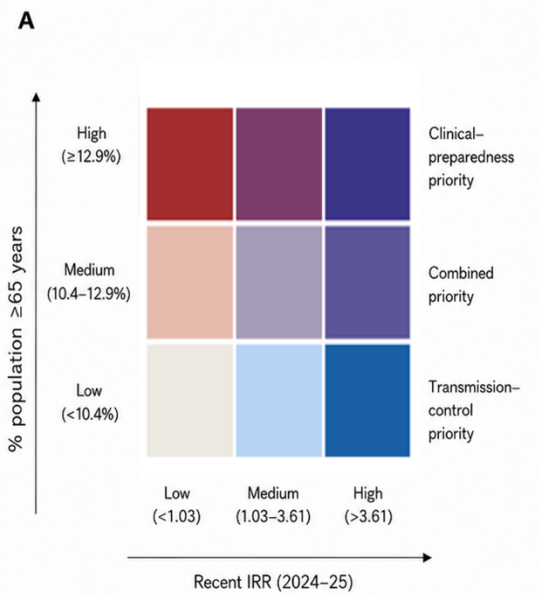

B

	Transmission–control priority	Clinical–preparedness priority	Combined priority
Municipal profile	High recent IRR + lower elderly share	Lower recent IRR + high elderly share	High recent IRR + high elderly share
Main question	Who to vaccinate?	Where to prep hospitals?	Do both
Recommended actions	• Prioritise vaccine deployment in municipalities with active or rising transmission • Focus on age groups with highest reported case burden (mainly adults 25–55 years), per local eligibility rules • Intensify vector control, diagnostics, and surveillance • Maintain routine hospital readiness	• Prepare hospitals, emergency care, and referral pathways in municipalities with older populations • Prioritise triage and early monitoring for older adults, especially men • Pre–position beds, IV fluids, diagnostics, and risk communication • Use vaccination selectively, weighing IXCHIQ safety concerns in adults ≥60 years	• Dual strategy: targeted vaccination + hospital surge preparation • Consider selective vaccination where transmission risk is high and benefit–risk is favorable • Expand referral capacity and clinical monitoring for older adults • Intensify surveillance and vector control

Figure S8. Decision-maker reference for the municipality-level chikungunya vaccination framework, Brazil, 2024–25. (A) Municipality classification using the Figure 6 axes: recent posterior incidence rate ratio (IRR) relative to the national municipality median in 2024–25 (x-axis) and proportion of the municipal population aged ≥65 years (y-axis). Colors correspond to the three priority zones defined by joint empirical tertiles, as in Figure 6. Intermediate cells lean toward the nearest corner action package. (B) Recommended actions by priority zone, organized by municipal profile, the central planning question, and suggested public health responses. Uses the same tertile thresholds as Figure 6: recent IRR <1.03 (low), 1.03–3.61 (medium), >3.61 (high); proportion aged ≥65 years <10.4% (low), 10.4–12.9% (medium), >12.9% (high). This framework is a planning heuristic for SUS implementation; classifications should be updated as surveillance data accumulate and as post-rollout evidence on IXCHIQ safety in adults ≥60 years accrues.

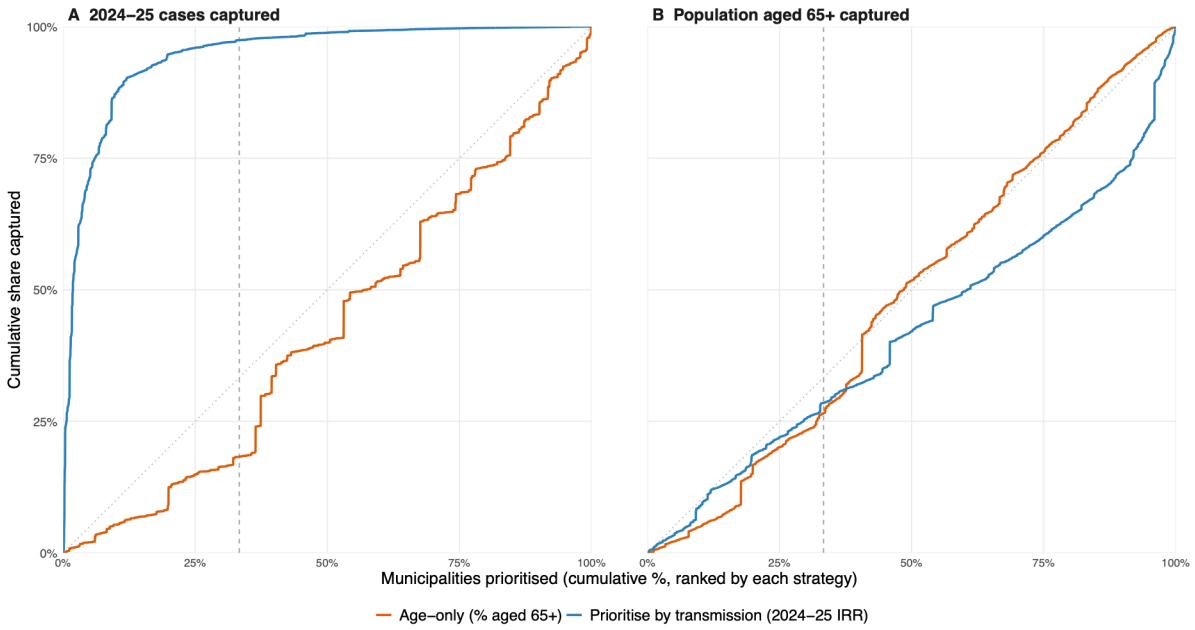

Figure S9. Cumulative capture of 2024–25 reported cases and population aged ≥65 years under two single-axis prioritization strategies, Brazil. (A) Cumulative share of 2024–25 confirmed chikungunya cases captured as municipalities are added in descending order of recent posterior IRR (transmission-priority rule, blue) or descending proportion of population aged ≥65 years (age-only rule, orange). (B) Cumulative share of population aged ≥65 years captured under the same two rankings. The dotted diagonal represents random prioritization; the dashed vertical line marks the top tertile threshold (33% of municipalities, n = 1,293). At that threshold, transmission-priority ranking captures 97% of 2024–25 reported cases versus 18% under age-only ranking (Panel A), whereas age-only ranking captures a substantially larger share of the population aged ≥65 years than transmission-priority ranking (Panel B); an age-targeted rule alone therefore leaves 82% of 2024–25 reported cases in municipalities it would not prioritize, which is the gap the transmission axis is designed to close. Neither single axis captures both dimensions simultaneously, motivating the joint targeting framework shown in Figure 6. Municipalities without model estimates (n = 1,691) are excluded. At matched coverage (the 1,293 municipalities constituting the upper tertile of elderly share, ≥12.9% aged ≥65 years), the framework's clinical-preparedness and combined zones select the same municipalities as an age-only rule and therefore capture an identical share of the severe-outcome-prone population — 26.6% weighted by population aged ≥65 years, and 21.1% weighted by observed 2024–25 deaths among those aged ≥65 years. These findings illustrate the complementary roles of the transmission and age axes, supporting the joint targeting framework shown in Figure 6.

Supplementary Tables

Table S1. Published chikungunya seroprevalence studies conducted in Brazil. The table summarizes study locations, survey periods, and target populations extracted from the literature.

City or area	Survey period (start to end)	Population type	Reference
Feira de Santana (George Américo)	2015-11 to 2015-12	General population (household-based)	[12]
Riachão do Jacuípe (Alto do Cemitério)	2015-11 to 2015-12	General population (household-based)	[12]
Feira de Santana (sentinel areas, urban)	2016-11 to 2017-09	General population (household-based, ≥1 year)	[13]
Macapá	2015-01 to 2015-05	Blood donors (volunteer)	[14]
Ribeirão Preto	2016-01 to 2016-05	Blood donors (volunteer)	[14]
São Sebastião	2020-02 to 2021-01	General population (household-based, ≥5 years)	[15]
Chapada district, Riachão do Jacuípe	2016-04 to 2016-04	General population (household-based, rural residents)	[16]
Fulni-ô Indigenous territory (Águas Belas / Itaíba)	2016-08 to 2017-06	Indigenous population (Fulni-ô tribe)	[17]
Truká Indigenous territory (Cabrobó / Ilha de Assunção)	2016-08 to 2017-06	Indigenous population (Truká tribe)	[17]
Juazeiro	2016-08 to 2017-06	General population (urban control)	[17]
Brasília (Federal District)	2019-01 to 2019-12	Blood donors (volunteer)	[18]
Diamantina	2018-01 to 2019-12	Pregnant women (asymptomatic cohort)	19
Rio de Janeiro city	2018-07 to 2018-10	General population (household-based)	[18]
Salvador (Pau da Lima community)	2016-11 to 2017-02	General population (household-based, ≥5 years)	[19]
Salvador	2017-09 to 2017-11	Postpartum women (asymptomatic cohort)	[19]
Quixadá	2018-06 to 2019-12	General population (household-based)	[20]

Table S2. Log-rank tests comparing time-to-event distributions along the chikungunya clinical pathway in Brazil. The table reports log-rank test results for differences in time-to-event distributions stratified by age group, sex, and race or ethnicity across three clinical intervals: symptom onset to hospitalization, hospitalization to death, and symptom onset to death. For each comparison, the number of groups, total sample size, chi-square statistic, degrees of freedom, and p-value are shown.

Interval	Stratification	χ^2 (df)	p-value
Onset to hospitalization	Age	12340 (9)	<2e-16
Onset to hospitalization	Sex	249 (1)	<2e-16
Onset to hospitalization	Race	442 (4)	<2e-16
Hospitalization to death	Age	1107 (9)	<2e-16
Hospitalization to death	Sex	28.8 (1)	8.12e-08
Hospitalization to death	Race	12.6 (4)	0.0136
Onset to death	Age	6216 (9)	<2e-16
Onset to death	Sex	114 (1)	<2e-16
Onset to death	Race	46.1 (4)	2.40E-09

Table S3. Cox proportional hazards models for demographic predictors of clinical progression among chikungunya cases in Brazil. The table reports hazard ratios (HRs) with 95% confidence intervals (CIs) and p-values for associations of age group, sex, and race or ethnicity with progression across three intervals: symptom onset to hospitalization, hospitalization to death, and symptom onset to death. The race reference group is Pardo (mixed), and age-specific estimates are shown relative to the 20–29 years reference category. Sensitivity analyses use white and Asian as alternative references

Age group (reference: 20-29-year)

Age group	Onset→hosp. HR (95% CI)	Hosp.→death HR (95% CI)	Onset→death HR (95% CI)
<1	8.87 (8.23–9.55)	1.62 (1.02–2.57)	18.95 (13.33–26.94)
1–9	4.30 (4.05–4.56)	0.295 (0.176–0.495)	1.685 (1.157–2.454)
10–19	1.556 (1.474–1.643)	0.710 (0.488–1.034)	1.314 (0.961–1.795)
30–39	0.923 (0.876–0.972)	1.026 (0.703–1.498)	1.051 (0.797–1.387)
40–49	0.858 (0.815–0.904)	1.415 (0.991–2.021)	1.401 (1.080–1.819)
50–59	0.940 (0.892–0.991)	1.715 (1.209–2.432)	2.459 (1.910–3.167)
60–69	1.228 (1.163–1.296)	2.941 (2.115–4.090)	4.637 (3.617–5.945)
70–79	2.133 (2.013–2.260)	5.698 (4.111–7.898)	13.91 (10.78–17.94)
≥80	4.453 (4.166–4.760)	10.57 (7.640–14.62)	50.77 (38.55–66.85)

Sex (reference: female)

Comparison	Onset to hosp. HR (95% CI)	Hosp. to death HR (95% CI)	Onset to death HR (95% CI)
Male vs Female	1.257 (1.222-1.294)	1.474 (1.278–1.700)	1.763 (1.587-1.959)

Race or ethnicity (reference: Pardo)

Group	Onset to hosp. HR (95% CI)	Hosp. to death HR (95% CI)	Onset to death HR (95% CI)
Asian	0.638 (0.539-0.755)	0.588 (0.189-1.830)	0.569 (0.283-1.141)
Black	0.840 (0.782-0.902)	0.901 (0.615-1.320)	0.751 (0.561-1.005)
Indigenous	1.490 (1.207-1.840)	0.344 (0.048-2.444)	0.779 (0.251-2.420)
White	1.374 (1.328-1.421)	1.277 (1.086-1.502)	1.468 (1.290-1.670)

Race or ethnicity (reference: white) - sensitivity

Group	Onset to hosp. HR (95% CI)	Hosp. to death HR (95% CI)	Onset to death HR (95% CI)
Asian	0.464 (0.392-0.551)	0.460 (0.147-1.438)	0.387 (0.192-0.781)
Black	0.611 (0.567-0.659)	0.705 (0.476-1.045)	0.512 (0.378-0.692)
Indigenous	1.085 (0.878-1.341)	0.269 (0.038-1.918)	0.531 (0.170-1.654)
Pardo (mixed)	0.728 (0.704-0.753)	0.783 (0.666-0.921)	0.681 (0.599-0.775)

Race or ethnicity (reference: Asian) - sensitivity

Group	Onset to hosp. HR (95% CI)	Hosp. to death HR (95% CI)	Onset to death HR (95% CI)
Black	1.316 (1.098-1.578)	1.533 (0.466-5.041)	1.320 (0.625-2.791)
Indigenous	2.337 (1.785-3.058)	0.584 (0.061-5.619)	1.370 (0.363-5.164)
Pardo (mixed)	1.568 (1.324-1.857)	1.701 (0.547-5.296)	1.759 (0.876-3.530)
White	2.153 (1.816-2.554)	2.173 (0.696-6.790)	2.581 (1.280-5.205)

Table S4. Comparison of key spatiotemporal model parameters between the primary Poisson specification and a negative binomial sensitivity analysis. CrI = credible interval. φ = proportion of total spatial variance attributable to structured spatial clustering. The negative binomial model showed improved fit by both DIC and WAIC, confirming overdispersion in municipality-month case counts. Estimates of φ, temporal precision, and the Zika covariate association were highly consistent across both specifications, supporting the robustness of the primary model conclusions.

Parameter	Poisson Mean	Poisson 95% CrI	NB Mean	NB 95% CrI
Spatial (BYM2): precision for space	0.450	0.413-0.485	0.397	0.365-0.429

Parameter	Poisson Mean	Poisson 95% CrI	NB Mean	NB 95% CrI
Spatial (BYM2): φ (structured spatial fraction)	0.699	0.649-0.755	0.693	0.641-0.744
Temporal (RW2): precision for time	4.295	3.515-5.248	4.196	3.194-5.442
Space-time interaction: precision for st_id	0.143	0.141-0.145	0.544	0.526-0.562
Zika covariate: exp(β) for Z_t	1.120	0.943-1.331	1.174	0.986-1.398
Overdispersion: size (1/overdispersion)	N/A	N/A	0.164	0.160-0.169
Model fit: DIC	806,237	-	484,146	-
Model fit: WAIC	1,945,718	-	470,086	-

Table S5. Macro-regional case fatality among hospitalized confirmed chikungunya cases by epidemic period and relative transmission intensity, Brazil, 2016–17 and 2024–25. Case fatality rate (CFR) was calculated as the number of deaths divided by the number of hospitalized confirmed cases within each macro-region and epidemic period. Relative transmission intensity reflects the macro-regional median posterior incidence rate ratio (IRR) from the Bayesian spatiotemporal model (Figure 2), categorized qualitatively as lowest, low, moderate, or highest relative to other macro-regions within the same epidemic period. During the first epidemic wave, the Northeast concentrated both the highest transmission intensity and the highest case fatality (6.36%). By the second wave, this alignment had broken: the Central-West had become the dominant high-transmission region but recorded a moderate case fatality (3.54%), while the Southeast, with moderate transmission intensity, had the highest case fatality (4.95%). Northeast case fatality fell to 1.38% despite the region's historically severe burden. This progressive spatial discordance between transmission and severity supports the demographic stratification described in the main text.

Macro-region	Epidemic period	Hospitalized confirmed cases	Deaths	CFR (%)	Relative transmission intensity
Central-West	Epidemic 1 (2016–17)	100	3	3.00	Low
Central-West	Epidemic 2 (2024–25)	2,285	81	3.54	Highest
North	Epidemic 1 (2016–17)	924	5	0.54	Moderate
North	Epidemic 2 (2024–25)	329	3	0.91	Moderate
Northeast	Epidemic 1 (2016–17)	2,926	186	6.36	Highest
Northeast	Epidemic 2 (2024–25)	1,592	22	1.38	Moderate

South	Epidemic 1 (2016–17)	17	0	0.00	Lowest
South	Epidemic 2 (2024–25)	461	14	3.04	Low
Southeast	Epidemic 1 (2016–17)	769	17	2.21	Low
Southeast	Epidemic 2 (2024–25)	3,291	163	4.95	Moderate

Table S6. Numbers at risk and censored observations for Kaplan-Meier survival analyses along the chikungunya clinical pathway, Brazil, 2015–2025. For each panel, numbers at risk (upper section) and interval-censored observations (lower section) are shown at selected time points for three sequential clinical intervals (symptom onset to hospitalization, hospitalization to death, and symptom onset to death), stratified by age group (Panel A), sex (Panel B), and race or ethnicity (Panel C). Time points are shown in days from the start of each interval. Individuals who did not experience the event of interest were right censored at the last observed date.

Panel A: Stratification by age group												
Number at Risk												
Age group	**Symptoms onset to hospitalization**				**Hospitalization to death**				**Symptoms onset to death**			
	t=0	**t=50**	**t=100**	**t=150**	**t=0**	**t=50**	**t=100**	**t=150**	**t=0**	**t=50**	**t=100**	**t=150**
<1	**10,860**	**9,861**	**9,857**	**9,855**	**1,010**	**341**	**213**	**190**	**10,860**	**10,163**	**10,034**	**10,010**
1–9	**65,999**	**62,963**	**62,939**	**62,934**	**3,068**	**867**	**470**	**384**	**65,999**	**63,785**	**63,384**	**63,298**
10–19	**137,999**	**135,692**	**135,662**	**135,655**	**2,356**	**692**	**305**	**233**	**137,999**	**136,312**	**135,924**	**135,852**
20–29	**200,314**	**198,141**	**198,124**	**198,123**	**2,204**	**567**	**242**	**173**	**200,314**	**198,660**	**198,331**	**198,262**
30–39	**212,144**	**210,028**	**210,006**	**209,998**	**2,155**	**582**	**226**	**175**	**212,144**	**210,547**	**210,189**	**210,138**
40–49	**209,744**	**207,799**	**207,776**	**207,773**	**1,983**	**526**	**195**	**138**	**209,744**	**208,255**	**207,918**	**207,861**
50–59	**178,679**	**176,864**	**176,841**	**176,837**	**1,849**	**504**	**189**	**126**	**178,679**	**177,269**	**176,944**	**176,880**
60–69	**125,580**	**123,911**	**123,894**	**123,889**	**1,695**	**429**	**150**	**113**	**125,580**	**124,234**	**123,951**	**123,912**
70–79	**66,348**	**64,820**	**64,809**	**64,807**	**1,548**	**381**	**135**	**97**	**66,348**	**65,067**	**64,815**	**64,773**

≥80	**26,736**	**25,465**	**25,456**	**25,454**	**1,285**	**263**	**91**	**68**	**26,736**	**25,561**	**25,372**	**25,344**
Number of Censored												
Age group	**Symptoms onset to hospitalization**				**Hospitalization to death**				**Symptoms onset to death**			
	t=0	**t=50**	**t=100**	**t=150**	**t=0**	**t=50**	**t=100**	**t=150**	**t=0**	**t=50**	**t=100**	**t=150**
<1	**0**	**0**	**0**	**0**	**12**	**629**	**124**	**23**	**12**	**629**	**124**	**23**
1–9	**0**	**0**	**0**	**0**	**32**	**2,173**	**383**	**82**	**32**	**2,173**	**383**	**82**
10–19	**0**	**0**	**0**	**0**	**19**	**1,625**	**378**	**69**	**19**	**1,625**	**378**	**69**
20–29	**0**	**0**	**0**	**0**	**35**	**1,587**	**303**	**65**	**35**	**1,587**	**303**	**65**
30–39	**0**	**0**	**0**	**0**	**53**	**1,495**	**340**	**52**	**53**	**1,495**	**340**	**52**
40–49	**0**	**0**	**0**	**0**	**35**	**1,382**	**320**	**56**	**35**	**1,382**	**320**	**56**
50–59	**0**	**0**	**0**	**0**	**31**	**1,272**	**299**	**62**	**31**	**1,272**	**299**	**62**
60–69	**0**	**0**	**0**	**0**	**22**	**1,167**	**266**	**35**	**22**	**1,167**	**266**	**35**
70–79	**0**	**0**	**0**	**0**	**19**	**1,016**	**224**	**35**	**19**	**1,016**	**224**	**35**
≥80	**0**	**0**	**0**	**0**	**15**	**788**	**158**	**22**	**15**	**788**	**158**	**22**
Panel B: Stratification by sex												
Number at Risk												
Sex	**Symptoms onset to hospitalization**				**Hospitalization to death**				**Symptoms onset to death**			
	t=0	**t=50**	**t=100**	**t=150**	**t=0**	**t=50**	**t=100**	**t=150**	**t=0**	**t=50**	**t=100**	**t=150**
Female	**756,502**	**745,998**	**745,887**	**745,859**	**10,693**	**2,869**	**1,206**	**895**	**756,502**	**748,414**	**746,722**	**746,405**
Male	**476,765**	**468,411**	**468,342**	**468,331**	**8,459**	**2,283**	**1,010**	**802**	**476,765**	**470,305**	**469,006**	**468,791**
Number of Censored												
Sex	**Symptoms onset to hospitalization**				**Hospitalization to death**				**Symptoms onset to death**			

	t=0	t=50	t=100	t=150	t=0	t=50	t=100	t=150	t=0	t=50	t=100	t=150
Female	**0**	**0**	**0**	**0**	**169**	**7,390**	**1,585**	**306**	**169**	**7,390**	**1,585**	**306**
Male	**0**	**0**	**0**	**0**	**104**	**5,743**	**1,210**	**195**	**104**	**5,743**	**1,210**	**195**
Panel C: Stratification by race or ethnicity												
Number at Risk												
Race &Ethnicity Group	**Symptoms onset to hospitalization**				**Hospitalization to death**				**Symptoms onset to death**			
	t=0	**t=50**	**t=100**	**t=150**	**t=0**	**t=50**	**t=100**	**t=150**	**t=0**	**t=50**	**t=100**	**t=150**
Pardo (Mixed)	**675,697**	**664,325**	**664,215**	**664,191**	**11,550**	**3,177**	**1,446**	**1,154**	**675,697**	**667,036**	**665,273**	**664,975**
Asian	**12,435**	**12,302**	**12,300**	**12,300**	**136**	**30**	**8**	**6**	**12,435**	**12,325**	**12,302**	**12,300**
Black	**56,554**	**55,762**	**55,751**	**55,748**	**813**	**230**	**92**	**69**	**56,554**	**55,954**	**55,814**	**55,790**
Indigenous	**3,426**	**3,343**	**3,341**	**3,340**	**87**	**14**	**7**	**6**	**3,426**	**3,351**	**3,344**	**3,343**
White	**199,586**	**194,978**	**194,939**	**194,931**	**4,672**	**1,164**	**414**	**287**	**199,586**	**195,985**	**195,225**	**195,096**
Number of Censored												
Race &Ethnicity Group	**Symptoms onset to hospitalization**				**Hospitalization to death**				**Symptoms onset to death**			
	t=0	**t=50**	**t=100**	**t=150**	**t=0**	**t=50**	**t=100**	**t=150**	**t=0**	**t=50**	**t=100**	**t=150**
Pardo (Mixed)	**0**	**0**	**0**	**0**	**157**	**7,886**	**1,643**	**282**	**157**	**7,886**	**1,643**	**282**
Asian	**0**	**0**	**0**	**0**	**2**	**103**	**20**	**2**	**2**	**103**	**20**	**2**
Black	**0**	**0**	**0**	**0**	**7**	**553**	**133**	**23**	**7**	**553**	**133**	**23**
Indigenous	**0**	**0**	**0**	**0**	**3**	**69**	**7**	**1**	**3**	**69**	**7**	**1**
White	**0**	**0**	**0**	**0**	**65**	**3,259**	**721**	**121**	**65**	**3,259**	**721**	**121**

Table S7. Macro-regional distribution of priority zones from the combined geographic and demographic targeting framework, Brazil, 2024 to 2025. Counts of Brazilian municipalities falling into each priority zone (transmission-control, clinical-preparedness, combined), stratified by macro-region. Zones are defined by joint empirical tertiles of recent (2024 to 2025) posterior incidence rate ratio and proportion of population aged 65 years and older (Figure 6). Equal column totals (832 transmission-control, 832 clinical-preparedness) are a mechanical consequence of the tertile classification rather than an empirical finding; macro-regional asymmetry within columns reflects the empirical patterns described in the main text.

Macro-region	Transmission control	Clinical preparedness	Both
North	63	9	3
Northeast	367	224	115
Central-West	208	33	39
Southeast	175	395	272
South	19	171	32
Total	**832**	**832**	**461**

Supplementary References:

1. Transferência de Arquivos – DATASUS. https://datasus.saude.gov.br/transferencia-de-arquivos/.
2. Estimativas da população residente para os municípios e para as unidades da federação | IBGE. https://www.ibge.gov.br/estatisticas/sociais/populacao/9103-estimativas-de-populacao.html.
3. Pereira, R. H. M. & Goncalves, C. N. geobr: Download Official Spatial Data Sets of Brazil. *CRAN: Contributed Packages* Preprint at https://doi.org/10.32614/CRAN.package.geobr (2019).
4. Cortes-Azuero, O. *et al.* The epidemiology of chikungunya virus in Brazil and the potential impact of vaccines: a mathematical modelling study. *Lancet Infect. Dis.* **26**, 406–416 (2026).
5. Travassos, C. & Williams, D. R. The concept and measurement of race and their relationship to public health: a review focused on Brazil and the United States. *Cad. Saude Publica* **20**, 660–678 (2004).
6. Torrence, C. & Compo, G. P. A Practical Guide to Wavelet Analysis. *Bull. Am. Meteorol. Soc.* **79**, 61–78 (1998).
7. Riebler, A. *et al.* An intuitive Bayesian spatial model for disease mapping that accounts for scaling. *Stat. Methods Med. Res.* **25**, 1145–1165 (2016).
8. MORAN, P. A. NOTES ON CONTINUOUS STOCHASTIC PHENOMENA. *Biometrika* **37**, 17–23 (1950).
9. Anselin, L. Local Indicators of Spatial Association—LISA. *Geogr. Anal.* **27**, 93–115 (1995).
10. Ver Hoef, J. M. & Boveng, P. L. Quasi-poisson vs. negative binomial regression: How should we model overdispersed count data? *Ecology* **88**, 2766–2772 (2007).
11. Santos, J. D. *et al.* Seroprevalence of Dengue, Chikungunya, and Zika viruses antibodies in a cohort of asymptomatic pregnant women in a low-income region of Minas Gerais, Brazil, 2018-2019. *Braz. J. Microbiol.* **54**, 1853–1858 (2023).